Characterization of Single Actomyosin Rigor Bonds: Load Dependence of Lifetime and Mechanical Properties

Takayuki Nishizaka,*† Ryuzo Seo,* Hisashi Tadakuma,* Kazuhiko Kinosita, Jr.,†‡ and Shin'ichi Ishiwata*†§¶

*Department of Physics, School of Science and Engineering, Waseda University, Tokyo169-8555; †Core Research for Evolutional Science and Technology, Genetic Programming Team 13, Kanagawa 216-0001; ‡Department of Physics, Faculty of Science and Technology, Keio University, Yokohama 223-8522; §Advanced Research Institute for Science and Engineering, Waseda University, Tokyo; and ¶Materials Research Laboratory for Bioscience and Photonics, Waseda University, Tokyo, Japan

ABSTRACT Load dependence of the lifetime of the rigor bonds formed between a single myosin molecule (either heavy meromyosin, HMM, or myosin subfragment-1, S1) and actin filament was examined in the absence of nucleotide by pulling the barbed end of the actin filament with optical tweezers. For S1, the relationship between the lifetime (τ) and the externally imposed load (F) at absolute temperature T could be expressed as $\tau(F) = \tau(0)\cdot\exp(-F\cdot d/k_BT)$ with $\tau(0)$ of 67 s and an apparent interaction distance d of 2.4 nm (k_B is the Boltzmann constant). The relationship for HMM was expressed by the sum of two exponentials, with two sets of $\tau(0)$ and d being, respectively, 62 s and 2.7 nm, and 950 s and 1.4 nm. The fast component of HMM coincides with $\tau(F)$ for S1, suggesting that the fast component corresponds to single-headed binding and the slow component to double-headed binding. These large interaction distances, which may be a common characteristic of motor proteins, are attributed to the geometry for applying an external load. The pulling experiment has also allowed direct estimation of the number of myosin molecules interacting with an actin filament. Actin filaments tethered to a single HMM molecule underwent extensive rotational Brownian motion, indicating a low torsional stiffness for HMM. From these results, we discuss the characteristics of interaction between actin and myosin, with the focus on the manner of binding of myosin.

INTRODUCTION

Recent developments in microscopic techniques have opened up opportunities of studying "single-molecule physiology," which enables us to elucidate protein-protein interactions and their various biological functions under living circumstances in aqueous media. For molecular motors, their individual behaviors have been successfully studied at the single molecule level. Nanometer steps and piconewton forces generated by single molecular motors have been measured under an optical microscope (Svoboda et al., 1993; Finer et al., 1994; Ishijima et al., 1994, 1998; Miyata et al., 1994, 1995; Molloy et al., 1995; Mehta et al., 1999). Single-fluorophore imaging (Funatsu et al., 1995; Sase et al., 1995a) has revealed individual ATP turnovers by myosin and rotational movement between actin and myosin (Sase et al., 1997), suggesting a hopping character for myosin (Kinosita et al., 1998). The mechanisms of motor operation, however, are still unclear. During one cycle of ATP hydrolysis, molecular motors are considered to form different conformations with different affinities for their substrate filaments and to alternate binding and unbinding. Here we focus on the characteristics of unbinding between myosin and actin.

In general, binding and unbinding interactions of proteins are essential for many biological functions, e.g., adhesion between cells, migration of cells on substratum (Nishizaka et al., 2000), recognition between ligands and receptors, processive movement of molecular motors, and so on. Several techniques have been developed to measure forces of protein bonds in the range from the subpiconewton level to a nanonewton. Glass microneedles were first applied to measure the sliding force generated between a microtubule and dynein motors (Kamimura and Takahashi, 1981) and then successfully used to measure the sliding force and the tensile strength of single actin filaments (Kishino and Yanagida, 1988; Tsuda et al., 1996). Individual ligand-receptor binding has been extensively characterized by atomic force microscopy (Nakajima et al., 1997; Fritz et al., 1998). The interaction between avidin and biotin has been examined in detail, and its molecular dynamics has been simulated (Florin et al., 1994; Moy et al., 1994; Grubmuller et al., 1996; Izrailev et al., 1997; Merkel et al., 1999). In the present study we used optical tweezers to characterize single actomyosin rigor bonds.

Optical tweezers, formed by focusing a laser beam, capture a particle of micrometer size without direct contact (Ashkin et al., 1986, 1990). In our previous studies (Nishizaka et al., 1995b), we measured the force required to unbind a rigor bond formed between an actin filament and a single heavy meromyosin (HMM) molecule in the absence of ATP using optical tweezers under a dual-view (fluorescence and phase-contrast) microscope (Kinosita et al., 1991; Sase et al., 1995b; Arai et al., 1999). The average unbinding force was ~9 pN, which is 2–5 times larger than the sliding force (Finer et al., 1994; Ishijima et al., 1994; Miyata et al., 1995) and an order of magnitude smaller than other intermolecular forces (Florin et al., 1994; Tsuda et al., 1996; Fritz et al., 1998). Unbinding under a constant force was a

Received for publication 28 February 2000 and in final form 26 April 2000.

Address reprint requests to Dr. Shin'ichi Ishiwata, Department of Physics, School of Science and Engineering, Waseda University, 3-4-1 Okubo, Shinjuku-ku, Tokyo 169-8555, Japan. Tel.: 81-3-5286-3437; Fax: 81-3-3200-2567; E-mail: ishiwata@mn.waseda.ac.jp.

0006-3495/00/08/962/13 $2.00

stochastic process, and an increase in the load by 10 pN decreased the lifetime of the rigor bond by a factor of 10^2 to 10^3. Interestingly, two types of HMM molecules were found, one with a large (long) and the other with a small (short) unbinding force (lifetime), suggesting "molecular individualism."

In this study, we measured the lifetime of single actomyosin (either HMM or subfragment-1 of myosin (S1)) rigor bonds under various external loads and could formulate the relationship between the lifetime and the load. The stochastic properties of the rigor bonds have been demonstrated. We developed a microscopic way to count the number of myosin molecules attached to the glass surface. Based on the number density of myosin molecules interacting with an actin filament thus measured, we estimated the minimum number of myosin molecules needed to slide actin filaments continuously. Furthermore, the torsional stiffness of single myosin molecules was estimated by observing the rotational Brownian motion of a short actin filament attached to myosin. Throughout the present study, we tried to characterize the interaction with actin of double-headed HMM molecules compared with that of single-headed S1 molecules.

MATERIALS AND METHODS

Dual-view imaging microscopy and optical tweezers system

Fig. 1 shows a schematic diagram of a dual-view (phase-contrast and fluorescence) video microscope imaging system (Kinosita et al., 1991; Nishizaka et al., 1995a,b; Sase et al., 1995b; Arai et al., 1999) equipped with optical tweezers. The inverted microscope (TMD-300; Nikon Co., Tokyo) with a 100× objective with a phase-contrast plate (NA 1.3, fluor 100 Ph; Nikon) was used on an optical bench (HG-LM; Herz Co., Kanagawa, Japan). The optical system included dichroic mirrors (DM 550, DM infrared, Sigma Koki Co., Saitama, Japan; DM 530, Asahi Spectra Co., Tokyo), filters (F 380–520, F 550, F 590; Asahi Spectra), and mirrors. The beam from the sample, which consisted of two components, the phase-contrast image of the bead (wavelength 380–520 nm, the *once-broken* line in Fig. 1) and the fluorescence image of actin filaments (excitation 550 nm and emission > 590 nm; the *dashed line* in Fig. 1), was separated by a beam separator (DM > 530 nm). Colorless filters (HA-30; Hoya Co., Tokyo, and Asahi Spectra) were placed behind the Hg lamp and before the image intensifier to cut off the infrared light. The field stop was positioned between the microscope and the beam separator, and lenses (DLB-50–150PM; Sigma Koki) were positioned before each camera to focus images clearly. The bead image, acquired with a CCD camera (CCD-72; Dage-MTI, Michigan City, IN), was stored in a digital frame memory (DIPS-C2000; Hamamatsu Photonics K. K., Hamamatsu, Japan). The position of the bead was determined by calculating the centroid of its intensity profile with a spatial resolution of nanometer scale (Fig. 2; Miyata et al., 1994; Nishizaka et al., 1995b). The data were analyzed with a personal computer (Apple Japan, Tokyo).

The sample stage of the microscope was replaced with the custom-made stage, on which the position of the objective along the *z* direction could be controlled by using a piezoelectric microscope positioner (P-720.00; Physik Instrumente GmbH and Co., Waldbronn, Germany) with a power supply (BWS 1202.5; Takasago, Tokyo). Because the drift between the commercial sample stage and the objective is mainly caused by deformation of the gear(s) sustaining a nose piece, the nose piece was removed and the objective was fixed directly to the sample stage to suppress the drift during measurements. Large displacement of the stage (as much as >40 nm) was achieved with the use of high-resolution actuators (HPA-10; Sigma Koki), their controller (Mark-8; Sigma Koki), and a personal computer (Apple Japan, Tokyo) with GPIB (NI488.2; National Instruments Co., Austin, TX). The small displacement (nanometer scale) was adjusted with a piezoelectric substage (p-770.10; Physik Instrumente GmbH and Co.) with a function generator (1915; NF Electronic Instruments, Yokohama, Japan) and an amplifier (BWS 120–2.5; Takasago). The temperature of the microscopic system was stabilized by allowing it to sit for 4–6 h before the measurements.

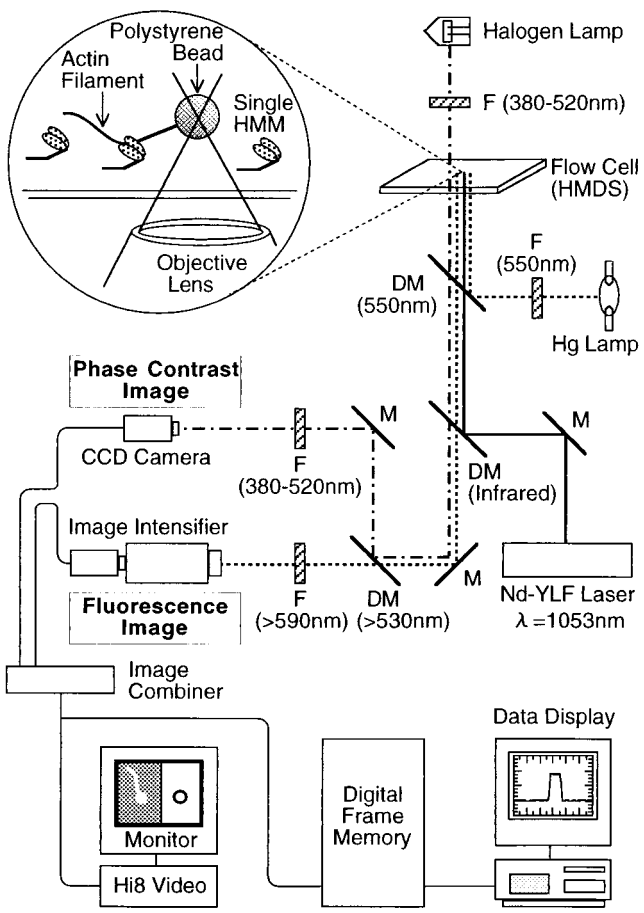

FIGURE 1 Schematic diagram of optical tweezers and dual-view imaging video microscope system. The once-broken lines and the dashed lines represent phase-contrast and fluorescence imaging optical paths, respectively, and the solid lines represent the optical tweezers optical path. The microscope system includes dichroic mirrors (DM) (the wavelength in parentheses shows the wavelength of the reflected light, and the wavelength with the > sign shows the range of wavelength passing through DM), filters (F) (the wavelength in parentheses shows the wavelength of light passing through F), and mirrors (M).

The spatial resolution of the system and the performance of the sample stage were examined by the method shown in Fig. 2. Fig. 2 *A* gives an example showing the position fluctuation of a bead trapped by optical tweezers with a stiffness of 0.27 pN/nm. The standard deviation (SD) of the displacement of the bead trapped for 1 min was 0.84 nm for the *x* direction and 0.93 nm for the *y* direction ($n = 5$). Here these values are considered to be the spatial resolution of our system, with 1/30 s time resolution. In

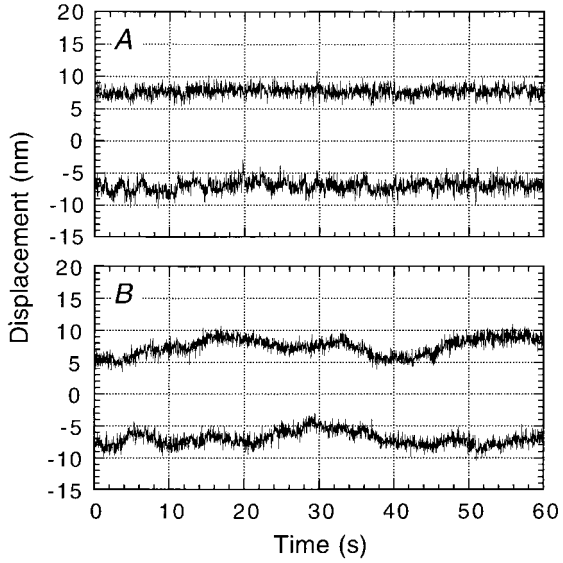

FIGURE 2 Performance of the image analysis system and the sample stage. (*A*) Time course of the displacement of the bead that was trapped in the medium by optical tweezers with a stiffness of 0.27 pN/nm. The displacement reflects both the stability of the trap center and the spatial resolution of our analysis system. (*B*) Displacement of the bead that was fixed to the glass surface. The glass surface was covered with nitrocellulose over the bead, so that the bead was fixed between the nitrocellulose membrane and the glass surface. Thus the displacement of the bead reflects the movement of the sample stage. Upper and lower traces in each figure respectively represent the displacements along the *x* and *y* axes.

contrast, to check the drift of the stage, we measured the displacement of the bead fixed to a glass surface by covering it with nitrocellulose (Fig. 2 *B*). The SD of the displacement of the bead for 1 min was 2.1 nm for the *x* direction and 2.0 nm for the *y* direction ($n = 10$). They were larger than the spatial resolution of our system, indicating the drift of the microscopic stage or the vibration of the system.

The actin filaments labeled with a fluorescent probe were visualized using another CCD camera equipped with an image intensifier (KS1381; Video Scope International, Washington, D.C.). To observe a phase-contrast image of beads simultaneously, the focus of the phase-contrast image plane was displaced ~0.5 μm (the radius of the bead) higher than the focus of the fluorescence image plane by moving the lenses in front of the camera. Two images were electronically combined (MV24-c; For. A Co., Tokyo) on the same screen to compare the behavior of the actin filament against the displacement of the bead at the same time.

The 1 W Nd:YLF laser (1053–1000p: $\lambda = 1.053$ μm; Amoco Laser Co., Naperville, IL) was coupled with an optical fiber, and the laser was not placed on the optical bench, to avoid a vibration. The position of the optical fiber could be moved along three directions (*x*, *y*, and *z*) and tilted in two directions (*xy* plane). The laser beam was set parallel with the objective (YTL-25-20PY1; Sigma Koki) and then focused with a custom-made optical apparatus (Nikon and Sigma Koki). The laser beam was led into the microscope from the right-hand side to the position just below the dichroic mirror for fluorescence excitation, which was originally designed to set an analyzer of a DIC microscope. The linear polarization of the laser light was changed to a circular polarization with a quarter wave plate. The laser light could be split into two beams with a set of beam splitters (PBN-20-16040; Sigma Koki) if needed. The trap stiffness we used, 0.1–0.3 pN/nm, was calibrated as described before (Nishizaka et al., 1995b).

In vitro assay system and preparation of bead-tailed F-actin

Actin and myosin were prepared from rabbit skeletal white muscle according to a standard procedure (Kondo and Ishiwata, 1976). HMM prepared by chymotryptic digestion, and s1 by papin digestion of myosin was stored in liquid N_2 (Nishizaka et al., 1993). A bead-tailed actin filament was prepared as previously reported (Suzuki et al., 1996). Bovine plasma gelsolin (Kurokawa et al., 1990) was cross-linked to the carboxylated polystyrene bead (1-μm diameter; Polysciences, Warrington, PA) with 1-ethyl-3-(3-dimethyl-aminopropyl)-carbodiimide (Nacalai Tesque Co., Kyoto), such that the barbed end (B-end) of an actin filament, which corresponds to the rear end when the filament slides, was attached to the bead. The average number of actin filaments attached to the bead was controlled by cross-linking an appropriate amount of bovine serum albumin (BSA) to the bead (BSA/gelsolin = 20:1 w/w). BSA labeled with rhodamine X maleimide (Molecular Probes, Eugene, OR) was also attached to the bead surface to visualize the bead as a fluorescence image (cold BSA/labeled BSA = 19:1). The bead was washed with F-buffer (0.1 M KCl, 2 mM $MgCl_2$, 2 mM 3-(*N*-morpholino)propanesulfonic acid (pH 7.0), 1.5 mM NaN_3, 1 mM dithiothreitol (DTT)) and mixed with 0.2 mg/ml actin filament labeled with rhodamine phalloidin (Molecular Probes) (Yanagida et al., 1984). Before infusion to the flow cell, bead-tailed actin filaments were diluted in F-buffer containing 1 mg/ml BSA to avoid adsorption of the bead to the glass surface. The in vitro assay system was prepared according to the report by Toyoshima et al. (1987), with slight modifications (Nishizaka et al., 1995b). The coverslip, cleaned in a sonicator with neutral detergent, was silanized with hexamethyl disilazane (Nacalai Tesque) (Nishizaka et al., 1995b). HMM and S1 were diluted in an assay buffer (AB) (25 mM KCl, 4 mM $MgCl_2$, 25 mM imidazole-HCl (pH 7.4), 1 mM EGTA, 1 mM DTT) and infused with the flow cell from one side and then from the other side after 60 s. The cell was washed with AB-buffer containing 0.5 mg/ml BSA, 10 mM DTT, 0.22 mg/ml glucose oxidase, 0.036 mg/ml catalase, and 4.5 mg/ml glucose. The bead-tailed actin filament, which was a mixture of 20 nM actin and 0.05% (w/v) bead, was infused. After washing with 3 volumes of AB-buffer containing 0.5 mg/ml BSA and the oxygen scavenger system, the edges of the flow cell were sealed with grease (Toray Dow Corning Silicone, Tokyo). All experiments were done at 30–32°C, except the S1 measurement at 27–32°C.

RESULTS

Direct counting of the number of HMM molecules

First we developed a method for directly counting the number of HMM molecules interacting with actin filaments. Our previous studies showed that the location of each HMM molecule attaching to a glass surface could be determined (Nishizaka et al., 1995a,b). When an actin filament was pulled and taut, HMM molecules could be recognized as a nodal point of the fluctuation of actin filament. By imposing the external load, we broke the nodal point and loosened the filament again (figure 1 *A* of Nishizaka et al., 1995a). Although this technique was useful for determining the location of HMM molecules, it was restricted to a very low density of HMM molecules, because the loosened part of the actin filament immediately attached to adjacent HMM molecules when the distance between adjacent molecules was less than ~1 μm. To solve this difficulty, the bead was manipulated not in the direction parallel to the glass surface but perpendicular to the surface (Figs. 3 and 4). This tech-

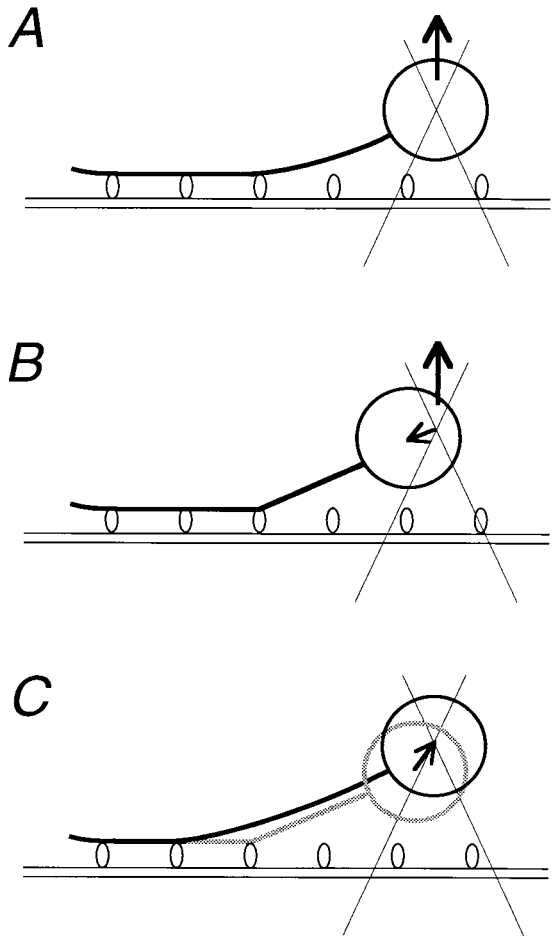

FIGURE 3 Schematic illustration of the technique used to count the number of motor molecules attached to the glass surface. The bead-tailed actin filament bound to HMM molecules was manipulated in the upward (*z*) direction at a constant rate (*A*). The filament was pulled taut from the HMM molecule (*B*), so that the bead was displaced from the trap center in the direction of the HMM. The bead returned to the trap center when the cross-bridge was broken, and subsequently the actin filament was loosened (*C*).

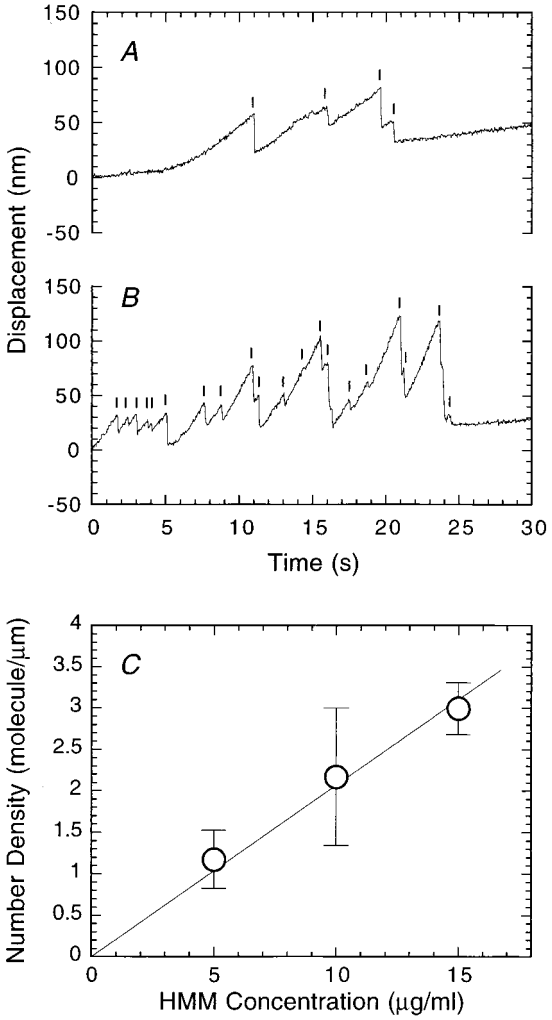

FIGURE 4 (*A* and *B*) Examples of the time course of the bead displacement projected onto the *xy* plane of the glass surface. The objective was moved in the upward (*z*) direction at a constant rate, 100 nm/s. The glass surface was precoated with 5 and 15 μg/ml HMM in *A* and *B*, respectively. The small bar indicates the moment at which the cross-bridge was broken (cf. Fig. 3 *C*). (*C*) The relation between the concentration of HMM infused into the flow cell and the number density of HMM. Bars indicate the standard deviation (n = 4–5). The slope of a linear approximation is 0.21 molecules/((μg/ml)·μm actin filament).

nique could be used to avoid overcounting the number of molecules.

Fig. 4, *A* and *B*, shows examples of the time course of the bead movement projected onto the *xy* plane with this technique. The trapped bead was manipulated in the upper *z* direction at a constant rate of 100 nm/s by moving the objective with a piezoelectric positioner (Fig. 3 *A*). After the part of the actin filament closest to the bead became taut, the bead began to deviate from the trap center (*sawtooth pattern* in Fig. 4, *A* and *B*; cf. Fig. 3 *B*). Then, after a while, the bead returned to the trap center accompanying the unbinding of the rigor bond. Thus each peak in Fig. 4, *A* and *B*, indicated by a small bar corresponds to the moment at which the cross-bridge was broken (Fig. 3 *C*). Finally, the filament was completely detached from the glass surface (at 21 s in Fig. 4 *A* and 24 s in Fig. 4 *B*). In 0–5 s and 21–30 s in Fig. 4 *A*, the trapped bead was displaced to the *x* direction at a rate of ~2 nm/s, which was accompanied by the upward motion of the objective. This movement is attributable to a slight misalignment between the laser beam and the optical center axis of the objective.

We applied the above method to the HMM solution in the range of 5–15 μg/ml (Fig. 4); at higher HMM concentrations, actin filaments were severed at a nodal point by pulling. The maximum trapping force of our system was estimated to be ~60 pN, indicating that an actin filament can be broken by applying a force less than 60 pN when the

filament is bent at an acute angle (cf. Arai et al., 1999). As shown in Fig. 4 *C*, the average number of HMM molecules that attached to a unit length of an actin filament was proportional to the concentration of infused HMM, and its slope was 0.21 molecules/((μg/ml)·μm actin filament).

We also examined the minimum concentration of HMM needed to achieve smooth sliding movement of actin filaments in the presence of 1 mM ATP. On the glass surface coated with HMM lower than 20 μg/ml, actin filaments could not slide and became detached from the glass surface. At 30 μg/ml HMM, actin filaments ~10 μm in length slid continuously at a speed of 9.3 ± 0.7 μm/s (n = 5), whereas short actin filaments slid intermittently and sometimes became detached. Under these conditions (1 mM ATP and 30 μg/ml HMM), the minimum length of actin filaments that slid continuously for 10 s was 1.4 μm.

Swiveling motion of actin filaments tethered to HMM

On a glass surface that was coated with a low concentration of HMM in the absence of ATP, short actin filaments (1–2 μm long) showed swiveling Brownian motion around a single point over a range of more than 360° (Nishizaka et al., 1995a,b). An example of this swiveling motion is shown in Fig. 7. This observation is analogous to the case of a microtubule tethered by a single kinesin molecule (Hunt and Howard, 1993). By analyzing the swiveling motion of actin filaments, we estimated the torsional stiffness of the flexible part, which is probably located in a HMM molecule.

The direction of a rotating actin filament was estimated from the centroid of its fluorescence image. We chose those actin filaments tethered to the glass surface by a single point that was slightly deviated from the center of the filament. When the filament swiveled around the tether point, the centroid of its fluorescence image also swiveled, showing the direction of the filament (Noji et al., 1997; Yasuda et al., 1998). Before the centroid calculation, noise in the video images was reduced by recording by averaging over 4 consecutive video frames. Actin filaments 1–3 μm long were selected for calculation to avoid the effect of their bending motion in calculation.

Fig. 5 *A* is an example showing the time course of the rotation of the short actin filament. The direction of the filament fluctuated with time. This fluctuation was assumed to be caused by thermal energy, and the torsional stiffness could be estimated as follows: the direction was divided every 1-rad partition, and the probability that the filament existed in each direction of 1 rad width, $P(\theta)$ (θ = torsion angle), was calculated. The energy $E(\theta)$ was thus obtained by the equation $E(\theta) = -k_B T \cdot \ln(P(\theta))$ as shown in Fig. 5 *B*, where k_B is the Boltzmann constant and T is the absolute temperature. The approximation of $E(\theta)$ to a spring shape function, $E(\theta) = \frac{1}{2} k \theta^2$ (k is the spring constant), is shown as a thin line in Fig. 5 *B*. The value of k was estimated to be

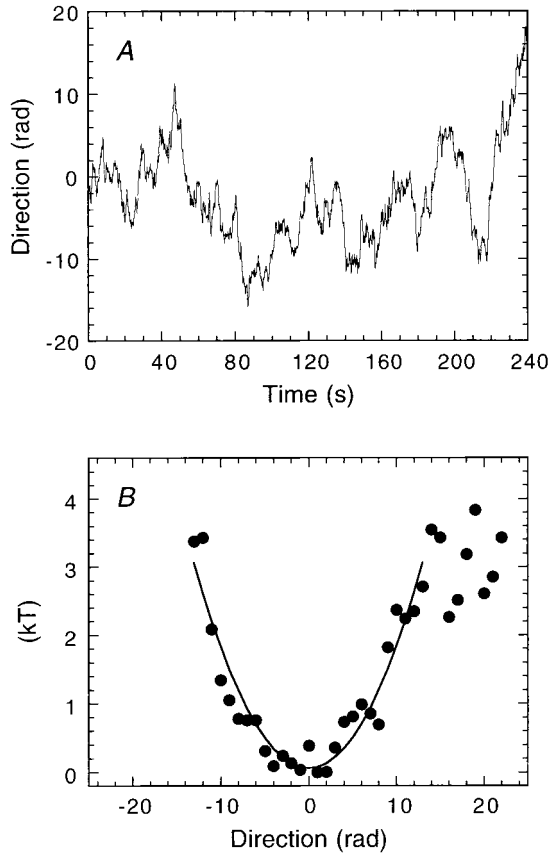

FIGURE 5 (*A*) An example showing the time course of swiveling of a short actin filament tethered to the glass surface through a single HMM molecule (see the short actin filament in Fig. 7, indicated by an *arrow*). (*B*) The energy profile showing the torsional stiffness of the single HMM molecule estimated from *A*. The thin line is an approximation with a spring shape function ($E(\theta) = 1/2 \cdot k\theta^2$, where $E(\theta)$ is energy, k is the spring constant, and θ is the torsion angle), in which the spring constant is 0.074×10^{-21} N · m/rad in the range of ±12 rad.

$2.3 \pm 1.9 \times 10^{-22}$ (± SD, n = 5) N·m/rad. Actin filaments rotated 6.4 times at maximum and 3.8 times on average.

Lifetime of single rigor bonds

In our previous studies (Nishizaka et al., 1995a,b), the unbinding force was measured by moving the trap center with a movable mirror. In the present study, the optical stage was displaced by using a piezoelectric substage, while the trap center was fixed. The advantage of this method is that the imposed load can be precisely determined at any moment. Fig. 6 illustrates how to examine the load dependence of the lifetime of single rigor bonds formed between a single actin filament and a single myosin (HMM or S1) molecule that attached to the glass surface. First the bead attached to the B-end of an actin filament is trapped by optical tweezers (Fig. 6 *A*). When the optical stage is displaced stepwise so as to make the actin filament taut, the

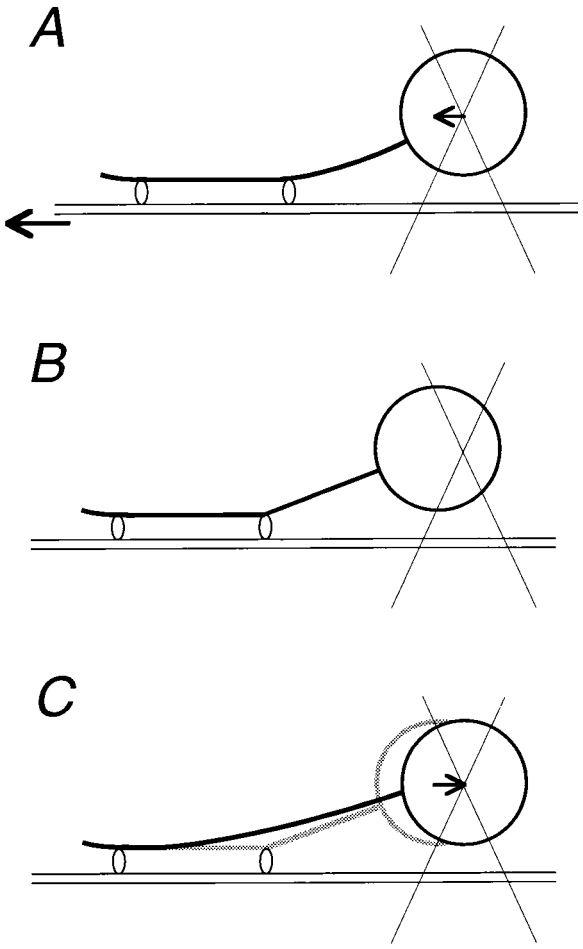

FIGURE 6 Schematic illustration of the procedure to measure the lifetime of the rigor bond between a single actin filament and a single HMM (or S1) molecule. (*A*) The bead-tailed actin filament bound to a motor protein is trapped by optical tweezers, and then the piezoelectric substage is displaced stepwise. (*B*) The filament is pulled taut from the motor protein, and the bead is displaced from the trap center, so that a sudden constant load is imposed on the rigor bond. (*C*) Finally, the bead returns to the trap center accompanying the breakage of the rigor bond, and the filament is loosened again. The time that elapsed between *B* and *C* corresponds to the lifetime of rigor bond.

bead is subsequently displaced from the trap center (Fig. 6, *A* and *B*). Thus a constant load is imposed stepwise on the rigor bond within a video frame, 1/30 s. After a while, the rigor bond is broken, and the bead is returned to the trap center (Fig. 6 *C*). The actin filament is loosened and shows bending Brownian motion again between the bead and the adjacent myosin molecule.

Fig. 7 is a series of fluorescence micrographs showing how to impose an external load on single rigor bonds. An actin filament was first trapped with optical tweezers (Fig. 7 *A*) and tautened by stepwise displacement to the left by the piezoelectric substage (Fig. 7 *B*) because the bead had located to the right of the HMM molecule. In this example, there were two HMM molecules that tethered the actin filament to the glass surface as identified as a nodal point (*arrowheads*), and the actin filament was pulled taut from the first HMM molecule. After a while, the bond was broken (Fig. 7 *C*), such that the lifetime of the rigor bond under a constant load could be directly measured. The actin filament was immediately loosened and showed bending Brownian motion again. When the stage was moved further, the filament was pulled taut from the next HMM molecule (Fig. 7 *D*). The stage was displaced stepwise again, and the second rigor bond was subsequently broken. Thus the actin filament was completely dissociated from the glass surface and the fluorescence image became out of focus (Fig. 7 *E*). Note that in Fig. 7, there is a short actin filament swiveling around a single point (indicated by a *small arrow*), at which a single HMM molecule is considered to be attached. The data in Fig. 5 were obtained from such a fluorescence image.

Fig. 8 *A* is an example of a record showing the time course of the displacement of the bead after stepwise imposition of an external load. When the stage was displaced stepwise (at 1.3 s, as shown by an *arrow*), the actin filament became taut (cf. Fig. 7, *B* and *D*), and the bead was displaced from the trap center. In this example, the external load imposed on the rigor bond was estimated to be 10.6 pN (we could not determine the external load beforehand, because the degree of loosening of an actin filament before applying the load could not be controlled), and the rigor bond was broken 0.43 s after the load was imposed. This observation showed that the lifetime of the actin-HMM rigor bond at no load, ~1000 s, was decreased to 0.43 s by imposing a load of 10.6 pN.

In the case of acto-S1 rigor bonds, spontaneous unbinding occurred, on the average, in ~100 s (Tadakuma et al., manuscript in preparation). Because of this short lifetime, measurement of the load dependence of the lifetime was technically difficult. To solve this problem, we prepared a flow cell coated with a higher density of S1 as compared with HMM, and actin filament was pulled at an acute angle to avoid the possibility of stretching two rigor bonds simultaneously.

Fig. 8 *B* is a summary showing the relationship between the imposed load and the lifetime. While the lifetime of HMM rigor bonds was distributed over a wide range of imposed loads, that of S1 rigor bonds was limited to a narrower range. In the case where a bond was broken within 66 ms (two video frames), we could not precisely determine the imposed load, so that these data (~5% of measurements) were omitted from Fig. 8 *B*. In the case of S1, there were four exceptional cases in which rigor bonds did not break for 60 s over 20 pN. We judge that they are attributable to the aggregation of S1, and thus they are not included in Fig. 8 *B*.

To elucidate the load dependence of the lifetime, we divided loads on the abscissa of Fig. 8 *B* into 3-pN partitions and replotted the time course of the unbinding occurrence of HMM and S1 rigor bonds in each partition, as shown in Fig. 9. The error bars indicate $N^{1/2}$, corresponding to the stan-

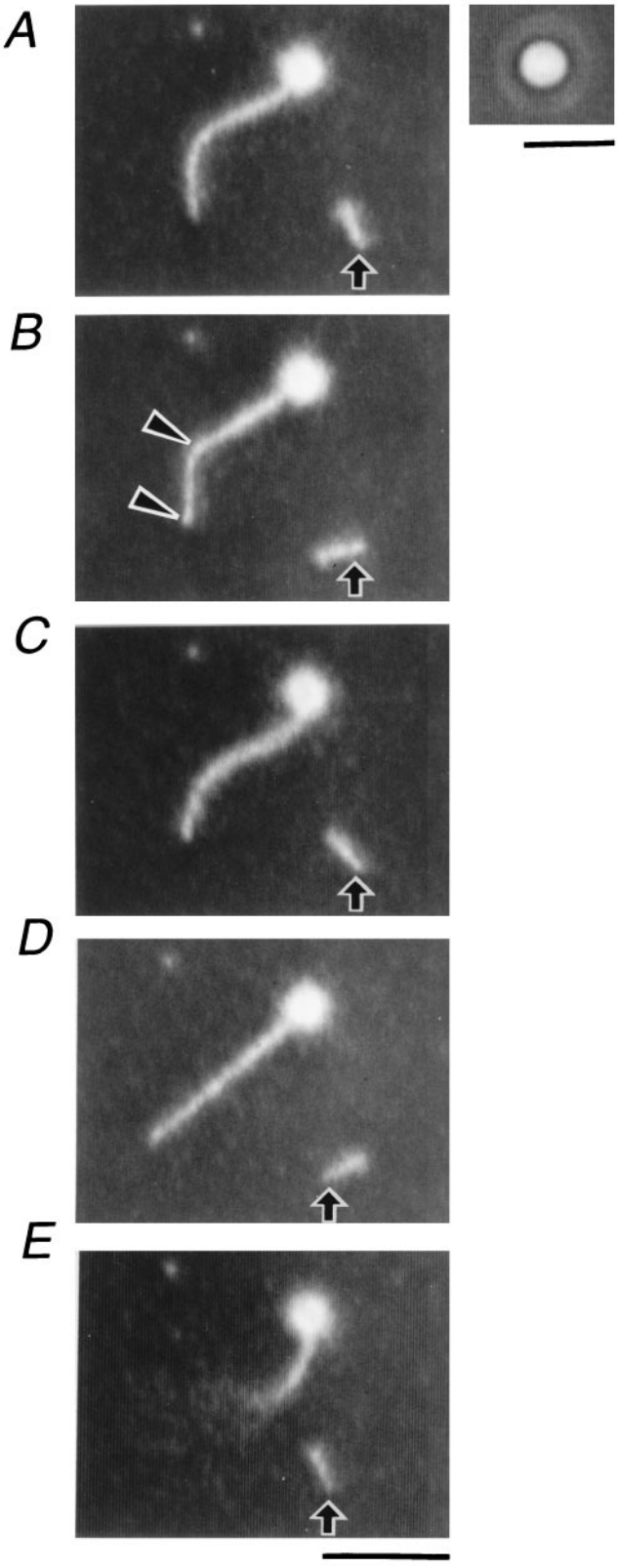

FIGURE 7 A series of fluorescence micrographs showing how to measure the lifetime of single rigor bond(s). (*A*) The bead attached to the B-end of an actin filament was trapped by optical tweezers. (*B*) The flow cell was moved (within 1/30 s) ~200 nm stepwise, using a piezoelectric substage, so that the actin filament was pulled taut from an HMM molecule (*arrowheads*). (*C*) After a while, the rigor bond was broken and the lifetime of the single rigor bond was measured. (*D*) The substage was moved further leftward and displaced stepwise again, such that the filament became nearly straight. (*E*) The filament was detached completely from the glass surface and showed Brownian motion. Note that a short actin filament, tethered to the glass surface through probably only one HMM molecule (indicated by an *arrow*), swiveled in each micrograph. Scale bar, 5 μm. (*upper right*) Phase-contrast image of the bead of *A–E*. Scale bar, 2 μm. The two images were simultaneously observed using the optics of Fig. 1.

dard deviation for events that stochastically occur N times. For S1, and for 9.0–12.0 pN and 12.0- pN of HMM, plots were approximated with the equation of a single exponential decay, $N(t) = N(0)\cdot\exp(-t/\tau)$, where τ is a lifetime of the rigor bond. Deviations of τ were estimated from fitted curves with maximum and minimum τ so as not to deviate from error bars by more than one data point in Fig. 9, and then they were expressed as error bars in Fig. 10. For 0.0–3.0, 3.0–6.0, and 6.0–9.0 pN of HMM, the data were approximated with the sum of two exponential decays, i.e., $N(t) = N_f(0)\cdot\exp(-t/\tau_f) + N_s(0)\cdot\exp(-t/\tau_s)$, where τ_f and τ_s are, respectively, a fast and a slow component of the lifetime, and $N_f(0) + N_s(0) = N_0$ is the total number of data at each region. After an optimum set of τ_f, τ_s, and $N_f(0)$ values was determined, deviations in τ_f and τ_s were independently estimated from fitted curves with maximum and minimum values so as not to deviate from the error bars of all data points. These maximum and minimum values of τ_f and τ_s were expressed as error bars in Fig. 10. The lifetimes thus obtained are summarized in Table 1.

Fig. 10 is a semilogarithmic plot of the data summarized in Table 1. As for the slow component of HMM, the relation between the lifetime, $\tau(F)$, and the imposed load, F, was closely approximated by the equation $\tau(F) = \tau(0)\cdot\exp(-F\cdot d/kT)$ (*thick solid line*). The relations for S1 and for the fast component of HMM were also approximated by this equation, as shown by a dashed line and a thin solid line, respectively. Note that the relation for S1 coincided with that for the fast component of HMM. From these approximation lines, d and $\tau(0)$ were estimated as summarized in Table 2.

DISCUSSION

Minimum number of HMM molecules needed to slide actin filaments continuously

The estimation of the number of myosin molecules interacting with an actin filament is essential for describing the sliding movement of an actin filament in an in vitro motility assay. Unlike myosin V (Mehta et al., 1999) or kinesin (Howard et al., 1989; Vale et al., 1996), the skeletal myosin (myosin II) molecule is not a processive motor, such that multiple motors are required for smooth and continuous

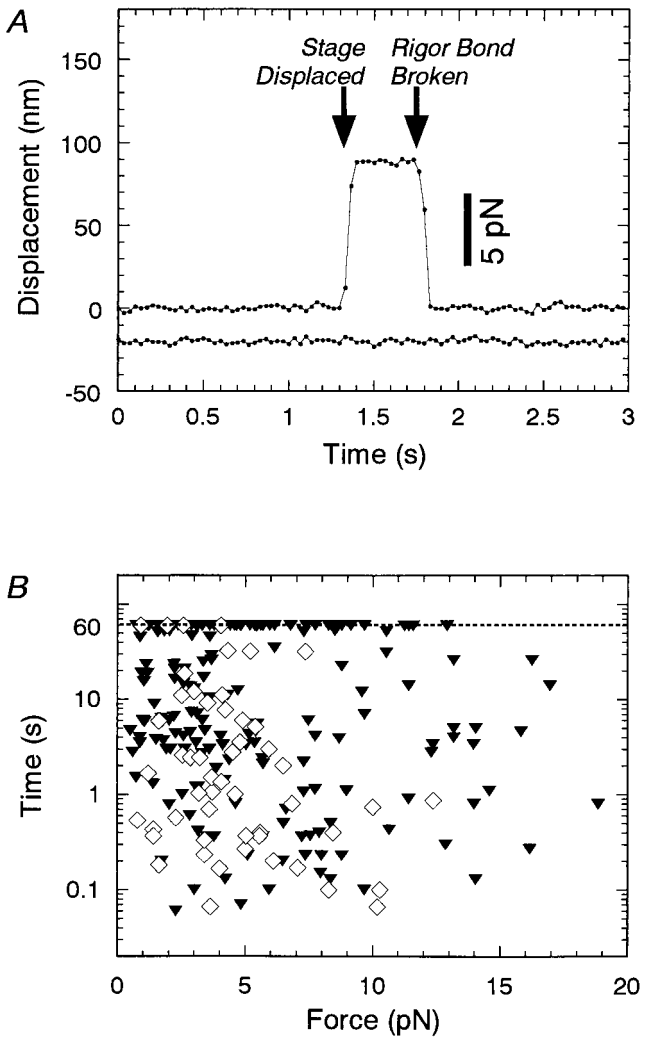

FIGURE 8 Load dependence of the lifetime of single rigor bonds. (*A*) An example of the time course of the displacement of the bead (cf. Figs. 6 and 7). Upper and lower plots show, respectively, the displacement of the bead along and perpendicular to the actin filament. Each dot was plotted every 1/30 s. The stage was displaced stepwise at 1.3 s so as to impose a constant external load, and then the bond was broken after 0.43 s in this example. (*B*) Relationship between the imposed load and the lifetime of rigor bonds of HMM (▼) and S1 (◇). For the rigor bonds not broken within 60 s, the lifetimes are plotted on the dashed line indicating 60 s.

sliding of actin filaments without dissociation. Although we could not directly count the number of HMM molecules during the sliding movement, the number required for smooth sliding of an actin filament could be estimated from our results (Fig. 4). The lowest concentration of HMM required for continuous sliding motion of actin filaments was 30 μg/ml in our method, so that the minimum line density of HMM molecules is estimated to be 30 (μg/ml) $\times$ 0.21 (molecules/μm/(μg/ml)) = 6.3 (molecules/μm actin filament). Furthermore, the minimum length of the filament showing the sliding movement was $\sim$1.4 μm under the same conditions. Thus we obtain the minimum number of molecules required for smooth sliding without dissociation, 6.3 (molecules/μm) $\times$ 1.4 (μm) = 8.8 (molecules).

We can assume that one ATP hydrolysis of the actomyosin system takes (10–100) ms, as in an in vitro motile system (Harada et al., 1990) and in solution (cf. Goldman, 1987). On the other hand, the probability that at least one myosin head binds to an actin filament is given by $P = 1 - \{(N - n)/N\}^N$, where N is the total number of myosin heads that can interact with the filament and n is the average number of heads that bind to the filament at one time. Therefore, $(1 - P) \times$ (10–100) ms is the dissociation period during which no myosin heads interact with the filament. The diffusion coefficient perpendicular to the filament axis for a 1.4-μm actin filament is calculated to be 1.4×10^{-8} cm^2/s from the equations $D = k_BT/\Gamma_\perp$ and $\Gamma_\perp = 4\pi\eta L/(\ln(L/2r) + \gamma_\perp)$, where $L = 1.4$ μm, $r = 5$ nm, $\eta = 0.010$ g/cm·s, $\gamma_\perp = 0.89$ (Hunt et al., 1994) and $T = 300$ K. Thus the time required for actin filaments 1.4 μm long to diffuse as far as δx, $\sim$17 nm (the size of myosin heads) to 34 nm (its doubled size), within which the filaments can maintain a sliding motion, is calculated to be 0.1–0.4 ms according to the equation $\delta x = (2Dt)^{1/2}$. To make $(1 - P) \times$ (10–100) ms shorter than 0.1–0.4 ms, P should be larger than 0.96–0.999. Together, n should be larger than 3.0–5.8 under $N = 17.6$ ($= 8.8 \times 2$) heads to keep P as 0.96–0.999 ($1 - \{(N - n)/N\}^N = 1 - \{(17.6–3.0)/17.6\}^{17.6} > 0.96$, $1 - \{(17.6–5.8)/17.6\}^{17.6} > 0.999$), suggesting that at least (3.0–5.8)/17.6 $\cong$ 17–30% of myosin heads always bind to the filament during sliding motion. If all n heads are in a state of producing the active force, the value 17–30% corresponds to the "duty ratio," which is the proportion of the period in which a single head produces the force in one ATPase cycle. However, because some head is only capable of holding the filament without producing active force (Goldman, 1987; Ishiwata and Yasuda, 1993), 17–30% could be an overestimation of the duty ratio.

Torsional stiffness of a single HMM molecule

By analysis of the rotational Brownian motion of a short actin filament tethered to a single HMM molecule, the torsional stiffness has been estimated to be $(2.3 \pm 1.9) \times 10^{-22}$ N·m/rad. The flexible part responsible for this small stiffness must be located at the joint between the S1 and S2 regions, and/or within the S2 region of the HMM molecule (Kinosita et al., 1984; Ishiwata et al., 1987, 1988). Note that this stiffness is so small that the thermal fluctuation energy, k_BT (4.1×10^{-21} N·m), can twist myosin 2.8 times ((4.1×10^{-21})/(2.3×10^{-22})/2π = 2.8). This small stiffness can explain the following mechanical properties of myosin previously reported: myosin can interact with an actin filament under various orientations (Toyoshima et al., 1989; Molloy et al., 1995), although it modifies the motor functions, such as the sliding velocity and force (Yamada et al., 1990; Sellers and Kachar, 1990; Ishijima et al., 1996). The unbinding

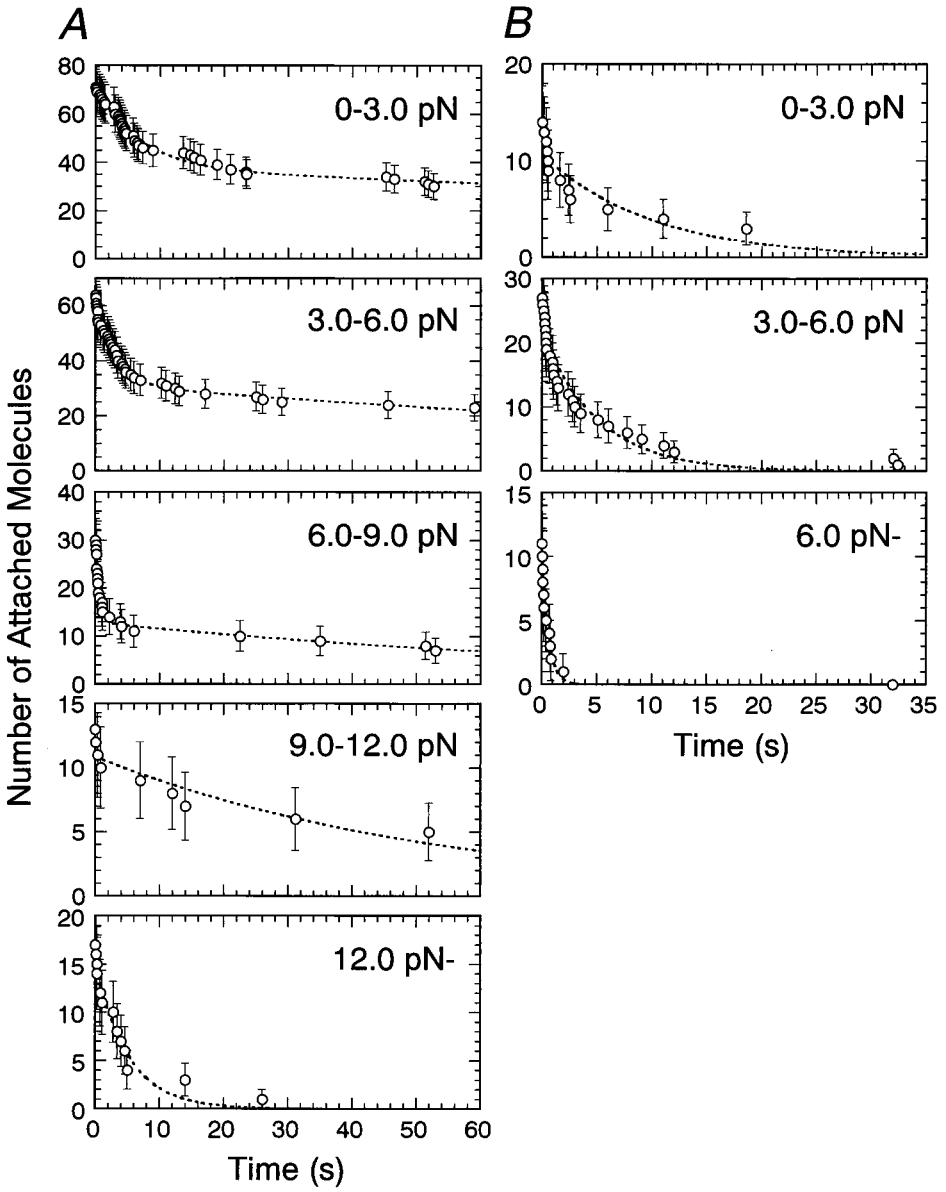

FIGURE 9 Time course of the decrease in the number of attached molecules, N, under various imposed loads, replotted from the data of Fig. 8 *B*. Error bars show standard deviation, which is simply determined as the square of the number of measurements at each point ($\pm N^{1/2}$). (*A*) HMM. Dashed lines indicate the approximation by $N(t) = N(0)\cdot\exp(-t/\tau)$ or $N(t) = N_f(0)\cdot\exp(-t/\tau_f) + N_s(0)\cdot\exp(-t/\tau_s)$ (for details see Results). (*B*) S1. Dashed lines indicate the approximation by $N(t) = N(0)\cdot\exp(-t/\tau)$.

force of rigor bonds is independent of the direction of external load, at least within ±90° (Nishizaka et al., 1995b). Because of the small stiffness, the geometrical relationship of the actin-myosin binding interface is probably maintained.

As for kinesin, the stiffness was estimated to be 1.2×10^{-22} N·m/rad by observing the rotational Brownian motion of an attached microtubule (Hunt and Howard, 1993), which is comparable to that of HMM. Thus such a small torsional stiffness may be common to motor proteins. Surprisingly, kinesin could be twisted more than 30 times by manipulation with optical tweezers without breaking the bond between kinesin and a microtubule (Kuo et al., 1995). This result may not be explainable by twisting of a head-rod junction; thus we alternatively assume that detachment and reattachment occur on one head while the other head binds to a filament. The twisting distortion in the attached head will be released during unbinding, and then the head can bind again without large distortion. If the two heads repeat this process alternately, the filament can rotate in one direction without limitation. We favor this model as an explanation of how protein can rotate more than 30 times without dissociation. If this process also occurred in our actin-HMM complex, the estimated value is an underestimation as a torsional stiffness of single HMM molecules.

Load dependence of lifetime of rigor bonds and binding manner of HMM

In our previous study, we repeatedly measured the load dependence of the lifetime of rigor bonds on the same

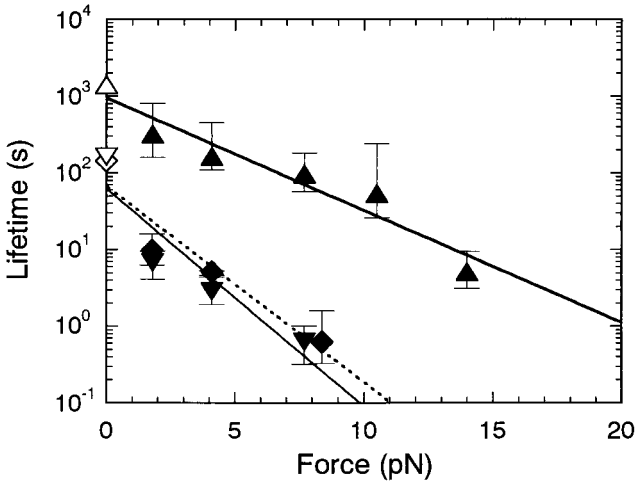

FIGURE 10 Relation between imposed load and lifetime of HMM and S1 rigor bonds. Triangles and inverted triangles show the slow and fast components of HMM, respectively. Squares show the lifetime of S1. Filled symbols were determined from Fig. 9, and open symbols are experimental data obtained without load (Tadakuma et al., manuscript in preparation). Fitted lines show the approximation by the equation $\tau(F) = \tau(0)\cdot\exp(-F\cdot d/k_BT)$. The thick and thin solid lines show the approximation of slow and fast components of HMM, respectively. The dashed line shows the approximation for S1.

acto-HMM rigor complexes (figure 4 in Nishizaka et al., 1995b). In the present study, we improved the mechanical stability of the microscopy apparatus to realize more accurate measurements, especially for longer times. As a result, the spatial resolution became less than 1 nm, and the drifting movement of the stage was restricted to within ~2 nm for 1 min. Such an improvement was essential for quantitatively investigating the relationship between the lifetime and the load.

TABLE 1 Lifetimes of HMM and S1 rigor bonds estimated from the approximation with exponential decay shown in Fig. 9

Load (pN)	Ratio, fast/total	Lifetime (s) τ_f	Lifetime (s) τ_s
A. HMM			
No load	(0.41)	(170)	(1400)
0–3	0.47	6.9	320
3–6	0.51	2.9	160
6–9	0.57	0.64	97
9–12	—	—	53
12+	—	—	5.1
	Lifetime (s)		
B. S1			
No load	(150)		
0–3	9.9		
3–6	5.2		
6–9	0.63		

The data were approximated by the equation of single exponential decay, $N(t) = N(0)\cdot\exp(-t/\tau)$, or the sum of two exponential decays, $N_f(0)\cdot\exp(-t/\tau_f) + N_s(0)\cdot\exp(-t/\tau_s)$. Ratio, $N_f(0)/(N_f(0) + N_s(0))$, means the proportion of cross-bridges having the fast component. Both ratio and lifetimes without load shown in parentheses were determined by the microscopic observation of spontaneous detachment from a glass surface of swiveling short actin filaments (Tadakuma et al., manuscript in preparation).

TABLE 2 Interaction distance, *d*, and lifetime without external load, $\tau(0)$, for, respectively, single rigor bonds of HMM and S1, estimated from the slope and the extrapolation of the solid and dashed lines in Fig. 10

	d	$\tau(0)$
HMM (fast)	2.7	62
HMM (slow)	1.4	950
S1	2.4	67

We found that the time course of the decrease in the number of attached S1 molecules under an external load nearly followed a single exponential decay (Fig. 9 *B*). In contrast, the decay for HMM was not expressed by a single exponential, except for a large applied force (Fig. 9 *A*), but could be approximated by the sum of two exponentials with different lifetimes. As shown in Table 1, *A* and *B*, the fast component of the lifetime of HMM nearly coincided with the lifetime of S1. One plausible explanation for this result is that HMM molecules that attached to the glass surface are classified into two groups: one having the slow component of lifetimes in which double-headed binding occurs, and another having the fast component in which only single-headed binding is possible, probably because of the adsorption of either head to the glass surface. This explanation will be examined in the future by using single-headed myosin (Harada et al., 1987) or single-headed HMM. The ratio between single-headed and double-headed molecules in our HMM assay is estimated to be nearly 1:1 (Table 1 *A*). We previously suggested the presence of "molecular individualism" in each HMM, based on the fact that each HMM molecule showed the individual load dependence of the lifetime (Nishizaka et al., 1995b). The difference in the number of active heads may be the main reason for this "individuality."

The lifetime, τ, is generally related to the activation energy for unbinding, $\Delta G^{\ddagger}$, through $\tau \propto \exp(\Delta G^{\ddagger}/k_BT)$. This could be extended to a fundamental property of the binding between a ligand and a receptor under an external load, i.e., $\tau(F) = \tau_0\cdot\exp((\Delta G^{\ddagger} - F\cdot d)/k_BT) = \tau(0)\cdot\exp(-F\cdot d/k_BT)$, where $\tau(F)$ is the lifetime under the load F and d is defined as the distance of an intermolecular interaction beyond which the intermolecular bond is ruptured (Bell, 1978; Erickson, 1994). The value of d is generally assumed to be less than a nanometer. Note that even though there is no load, the intermolecular bonds in an aqueous solution break with a lifetime of $\tau(0)$ in a stochastic manner under thermal equilibrium. This aspect is essential for understanding the unbinding force of the bond between proteins. The unbinding force between proteins was previously estimated to be

larger than 100 pN (Kishino and Yanagida, 1988; Florin et al., 1994; Tsuda et al., 1996; Fritz et al., 1998); however, it has been predicted that these values depend on the rate of the increase in the applied load. The unbinding force could be smaller when the external load is applied slowly, e.g., at a rate comparable to the dissociation rate constant. This was confirmed for actin-HMM rigor complex (cf. Fig. 4 in Nishizaka et al., (1995b)) and for avidin-biotin complex: the unbinding force increases from several piconewtons to hundreds of piconewtons as the velocity is increased by 10^6 (Merkel et al., 1999). In the case of P-selectin, the unbinding force was confirmed to increase logarithmically with the increase in the pulling velocities of ligand against receptor (figure 5 in Fritz et al., 1998). Thus the difference in the pulling velocity is considered to be the main reason why the average unbinding force of actin-HMM rigor complex obtained by AFM (Nakajima et al., 1997), ~14 pN, was larger than that obtained with optical tweezers (Nishizaka et al., 1995b), ~9 pN.

The exponential dependence of lifetime on the external load, which was predicted before (Bell, 1978; Erickson, 1994), fits well with our results as shown in Fig. 10. From the slope of the straight lines in Fig. 10, we obtained the values of d: 1.4 nm for the slow component of HMM, 2.7 nm for the fast component of HMM, and 2.4 nm for S1 (Table 2). The value of d for slow HMM components, which corresponds to the double-headed binding, was nearly one-half of those of d for fast HMM components, corresponding to the single-headed binding, and for S1. This difference by a factor of 2 suggests that the external load (F) is evenly shared on each attached head of HMM, such that the external load imposed on each head effectively becomes a half. This suggests that d for the interaction between single-head myosin and actin is ~2.5 nm.

It is expected that the large d value is attributable to the geometry of application of an external load. In fact, regarding the interaction between actin monomers in a filamentous actin, the tensile strength depends on the direction of the applied load to the molecular interface. Tsuda et al. (1996) reported that 600 pN was required for the breakage of the actin filament by straight pull, whereas Arai et al. (1999) reported that the actin filament broke when they applied 1 pN after tying a knot in it. In both measurements, the process of unbinding was observed at a video rate, so that the duration required for breakage was similar. Thus the apparent value of d for the latter may be an order of magnitude larger than that for the former.

In our system, the load was always imposed toward the long axis of an actin filament. The value of d could be decreased when the external load is applied in the direction parallel to the coordinate axis of the interaction potential, which may usually be the direction perpendicular to the intermolecular interface. The proposed structure of myosin head is longitudinally thin, and the actin-binding site is not located at the tip of the head but relatively at the side of the catalytic domain of the head, such that myosin heads bind to an actin filament at an acute angle (Rayment et al., 1993a,b). As a result, the myosin is being pulled from an angle, which would tend to tilt it out of the interface rather than pulling it out perpendicularly. The applied load could induce the distortion of the myosin head around the binding interface, then the activation energy for unbinding is efficiently decreased by a small load, as shown in Fig. 10, which results in the large value of d. In contrast, in the case of avidin-biotin unbinding force measurement by AFM (Florin et al., 1994; Moy et al., 1994), a symmetrical avidin molecule was sandwiched between an AFM cantilever and an agarose bead that was biotinylated (the 50-μm-diameter agarose bead versus the 6-nm-diameter avidin). It is expected that the load was imposed nearly perpendicularly to the interface of the avidin-biotin bond (Grubmuller et al., 1996; Evans and Ritchie, 1997; Izrailev et al., 1997), so that the small value of d was obtained.

X-ray crystallography showed that the myosin head consists of two domains, i.e., a catalytic domain that contains ATP- and actin-binding sites, and a neck domain. One possible hypothesis for how myosin heads generate force is that the neck domain tilts against the catalytic domain like a lever arm and induces a power stroke accompanied by the release of P_i (Rayment et al., 1993a,b; Corrie et al., 1999; Taylor et al., 1999). This structural dynamic is thought to be coupled with the change in the binding affinity between the myosin head and actin (Goldman and Brenner, 1987), although this hypothesis seems to have difficulty explaining the results showing their uncoupling (Ishijima et al., 1998) and multiple unitary displacements of single myosin head per ATP hydrolysis (Kitamura et al., 1999). In general, it is believed that the post-power stroke state has higher binding affinity for actin, and the pre-power stroke state has relatively lower affinity. In our experiments, the actin filament was always pulled in the direction of the reversal of the power stroke of myosin because the bead was attached to the B-end of an actin filament. In other words, we imposed the load so as to change the state of myosin from a post-power stroke state to a pre-power stroke state. If the structure of the myosin head changes from a high-affinity form to a low-affinity form with the application of an external load, the unbinding that occurs very efficiently with an imposed load can also be explained by this mechanism. In this relation, the following experiment is interesting: measurement of the lifetime by pushing the myosin head, which is in the pre-power stroke state with ATP analogs, toward the post-power stroke state along the direction of the power stroke. In this case, the lifetime may become longer because of the transition from the low-affinity state to the high-affinity state.

Finally, we would like to point out that the geometry for applying an external load in our system is similar to that in muscle fibers. The gradual change in the binding affinity, which is assumed in the Huxley and Simmons model (Hux-

ley and Simmons, 1971), may accompany the change in the number of intermolecular bonds at the actomyosin interface. Thus a large value of d may be a feature common to motor proteins.

We thank Drs. Naoya Suzuki, Hidetake Miyata, Ichiro Sase, and Ryohei Yasuda of Keio University and Mr. Madoka Suzuki of Waseda University for their technical support and advice. This research was partly supported by grants-in-aid for Scientific Research, for Scientific Research for Priority Areas, and for the High-Tech Research Center Project to SI from the Ministry of Education, Science, Sports and Culture of Japan, and by grants-in-aid from the Japan Science and Technology Corporation. TN was a Research Fellow of the Japan Society for the Promotion of Science.

REFERENCES

Arai, Y., R. Yasuda, K. Akashi, Y. Harada, H. Miyata, K. Kinosita, Jr., and H. Itoh. 1999. Tying a molecular knot with optical tweezers. *Nature.* 399:446–448.

Ashkin, A., J. M. Dziedzic, J. E. Bjorkholm, and S. Chu. 1986. Observation of a single-beam gradient force optical trap for dielectric particles. *Optics Lett.* 11:288–290.

Ashkin, A., K. Schutze, J. M. Dziedzic, U. Euteneuer, and M. Schliwa. 1990. Force generation of organelle transport measured in vivo by an infrared laser trap. *Nature.* 348:346–348.

Bell, G. I. 1978. Models for the specific adhesion of cells to cells. *Science.* 200:618–627.

Corrie, J. E., B. D. Brandmeier, R. E. Ferguson, D. R. Trentham, J. Kendrick-Jones, S. C. Hopkins, U. A. van der Heide, Y. E. Goldman, C. Sabido-David, R. E. Dale, S. Criddle, and M. Irving. 1999. Dynamic measurement of myosin light-chain-domain tilt and twist in muscle contraction. *Nature.* 400:425–430.

Erickson, H. P. 1994. Reversible unfolding of fibronectin type III and immunoglobulin domains provides the structural basis for stretch and elasticity of titin and fibronectin. *Proc. Natl. Acad. Sci. USA.* 91: 10114–10118.

Evans, E., and K. Ritchie. 1997. Dynamic strength of molecular adhesion bonds. *Biophys. J.* 72:1541–1555.

Finer, J. T., R. M. Simmons, and J. A. Spudich. 1994. Single myosin molecule mechanics: piconewton forces and nanometre steps. *Nature.* 368:113–119.

Florin, E. L., V. T. Moy, and H. E. Gaub. 1994. Adhesion forces between individual ligand-receptor pairs. *Science.* 264:415–417.

Fritz, J., A. G. Katopodis, F. Kolbinger, and D. Anselmetti. 1998. Force-mediated kinetics of single P-selectin/ligand complexes observed by atomic force microscopy. *Proc. Natl. Acad. Sci. USA.* 95:12283–12288.

Funatsu, T., Y. Harada, M. Tokunaga, K. Saito, and T. Yanagida. 1995. Imaging of single fluorescent molecules and individual ATP turnovers by single myosin molecules in aqueous solution. *Nature.* 374:555–559.

Goldman, Y. E. 1987. Kinetics of the actomyosin ATPase in muscle fibers. *Annu. Rev. Physiol.* 49:637–654.

Goldman, Y. E., and B. Brenner. 1987. Special topic: molecular mechanism of muscle contraction. General introduction. *Annu. Rev. Physiol.* 49:629–636.

Grubmuller, H., B. Heymann, and P. Tavan. 1996. Ligand binding: molecular mechanics calculation of the streptavidin-biotin rupture force. *Science.* 271:997–999.

Harada, Y., A. Noguchi, A. Kishino, and T. Yanagida. 1987. Sliding movement of single actin filaments on one-headed myosin filaments. *Nature.* 326:805–808.

Harada, Y., K. Sakurada, T. Aoki, D. D. Thomas, and T. Yanagida. 1990. Mechanochemical coupling in actomyosin energy transduction studied by in vitro movement assay. *J. Mol. Biol.* 216:49–68.

Howard, J., A. J. Hudspeth, and R. D. Vale. 1989. Movement of microtubules by single kinesin molecules. *Nature.* 342:154–158.

Hunt, A. J., F. Gittes, and J. Howard. 1994. The force exerted by a single kinesin molecule against a viscous load. *Biophys. J.* 67:766–781.

Hunt, A. J., and J. Howard. 1993. Kinesin swivels to permit microtubule movement in any direction. *Proc. Natl. Acad. Sci. USA.* 90: 11653–11657.

Huxley, A. F., and R. M. Simmons. 1971. Proposed mechanism of force generation in striated muscle. *Nature.* 233:533–538.

Ishijima, A., Y. Harada, H. Kojima, T. Funatsu, H. Higuchi, and T. Yanagida. 1994. Single-molecule analysis of the actomyosin motor using nano-manipulation. *Biochem. Biophys. Res. Commun.* 199: 1057–1063.

Ishijima, A., H. Kojima, T. Funatsu, M. Tokunaga, H. Higuchi, H. Tanaka, and T. Yanagida. 1998. Simultaneous observation of individual ATPase and mechanical events by a single myosin molecule during interaction with actin. *Cell.* 92:161–171.

Ishijima, A., H. Kojima, H. Higuchi, Y. Harada, T. Funatsu, and T. Yanagida. 1996. Multiple- and single-molecule analysis of the actomyosin motor by nanometer-piconewton manipulation with a microneedle: unitary steps and forces. *Biophys. J.* 70:383–400.

Ishiwata, S., K. Kinosita, Jr., H. Yoshimura, and A. Ikegami. 1987. Rotational motions of myosin heads in myofibril studied by phosphorescence anisotropy decay measurements. *J. Biol. Chem.* 262: 8314–8317.

Ishiwata, S., K. Kinosita, Jr., H. Yoshimura, and A. Ikegami. 1988. Optical anisotropy decay studies of the dynamic structure of myosin filaments. *Adv. Exp. Med. Biol.* 226:267–276.

Ishiwata, S., and K. Yasuda. 1993. Mechano-chemical coupling in spontaneous oscillatory contraction of muscle. *Phase Transitions.* 45: 105–136.

Izrailev, S., S. Stepaniants, M. Balsera, Y. Oono, and K. Schulten. 1997. Molecular dynamics study of unbinding of the avidin-biotin complex. *Biophys. J.* 72:1568–1581.

Kamimura, S., and K. Takahashi. 1981. Direct measurement of the force of microtubule sliding in flagella. *Nature.* 293:566–568.

Kinosita, K., Jr., S. Ishiwata, H. Yoshimura, H. Asai, and A. Ikegami. 1984. Submicrosecond and microsecond rotational motions of myosin head in solution and in myosin synthetic filaments as revealed by time-resolved optical anisotropy decay measurements. *Biochemistry.* 23:5963–5975.

Kinosita, K., Jr., H. Itoh, S. Ishiwata, K. Hirano, T. Nishizaka, and T. Hayakawa. 1991. Dual-view microscopy with a single camera: real-time imaging of molecular orientations and calcium. *J. Cell Biol.* 115:67–73.

Kinosita, K., Jr., R. Yasuda, H. Noji, S. Ishiwata, and M. Yoshida. 1998. F_1-ATPase: a rotary motor made of a single molecule. *Cell.* 93:21–24.

Kishino, A., and T. Yanagida. 1988. Force measurements by micromanipulation of a single actin filament by glass needles. *Nature.* 334:74–76.

Kitamura, K., M. Tokunaga, A. H. Iwane, and T. Yanagida. 1999. A single myosin head moves along an actin filament with regular steps of 5.3 nanometres. *Nature.* 397:129–134.

Kondo, H., and S. Ishiwata. 1976. Uni-directional growth of F-actin. *J. Biochem.* 79:159–171.

Kuo, S. C., K. Ramanathan, and B. Sorg. 1995. Single kinesin molecules stressed with optical tweezers. *Biophys. J.* 68:74s.

Kurokawa, H., W. Fujii, K. Ohmi, T. Sakurai, and Y. Nonomura. 1990. Simple and rapid purification of brevin. *Biochem. Biophys. Res. Commun.* 168:451–457.

Marston, S. B. 1982. The rates of formation and dissociation of actin-myosin complexes. Effects of solvent, temperature, nucleotide binding and head-head interactions. *Biochem. J.* 203:453–460.

Mehta, A. D., R. S. Rock, M. Rief, J. A. Spudich, M. S. Mooseker, and R. E. Cheney. 1999. Myosin-V is a processive actin-based motor. *Nature.* 400:590–593.

Merkel, R., P. Nassoy, A. Leung, K. Ritchie, and E. Evans. 1999. Energy landscapes of receptor-ligand bonds explored with dynamic force spectroscopy. *Nature.* 397:50–53.

Miyata, H., H. Hakozaki, H. Yoshikawa, N. Suzuki, K. Kinosita Jr, T. Nishizaka, and S. Ishiwata. 1994. Stepwise motion of an actin filament

over a small number of heavy meromyosin molecules is revealed in an in vitro motility assay. *J. Biochem.* 115:644–647.

Miyata, H., H. Yoshikawa, H. Hakozaki, N. Suzuki, T. Furuno, A. Ikegami, K. Kinosita, Jr., T. Nishizaka, and S. Ishiwata. 1995. Mechanical measurements of single actomyosin motor force. *Biophys. J.* 68:286s–290s.

Molloy, J. E., J. E. Burns, J. Kendrick-Jones, R. T. Tregear, and D. C. White. 1995. Movement and force produced by a single myosin head. *Nature.* 378:209–212.

Moy, V. T., E. L. Florin, and H. E. Gaub. 1994. Intermolecular forces and energies between ligands and receptors. *Science.* 266:257–259.

Nakajima, H., Y. Kunioka, K. Nakano, K. Shimizu, M. Seto, and T. Ando. 1997. Scanning force microscopy of the interaction events between a single molecule of heavy meromyosin and actin. *Biochem. Biophys. Res. Commun.* 234:178–182.

Nishizaka, T., H. Miyata, H. Yoshikawa, S. Ishiwata, and K. Kinosita, Jr. 1995a. Mechanical properties of single protein motor of muscle studied by optical tweezers. *Biophys. J.* 68:75s.

Nishizaka, T., H. Miyata, H. Yoshikawa, S. Ishiwata, and K. Kinosita, Jr. 1995b. Unbinding force of a single motor molecule of muscle measured using optical tweezers. *Nature.* 377:251–254.

Nishizaka, T., Q. Shi, and M. P. Sheetz. 2000. Position dependent linkages of fibronectin-integrin-cytoskeleton. *Proc. Natl. Acad. Sci. USA.* 97: 692–697.

Nishizaka, T., T. Yagi, Y. Tanaka, and S. Ishiwata. 1993. Right-handed rotation of an actin filament in an in vitro motile system. *Nature.* 361:269–271.

Noji, H., R. Yasuda, M. Yoshida, and K. Kinosita, Jr. 1997. Direct observation of the rotation of F_1-ATPase. *Nature.* 386:299–302.

Rayment, I., H. M. Holden, M. Whittaker, C. B. Yohn, M. Lorenz, K. C. Holmes, and R. A. Milligan. 1993a. Structure of the actin-myosin complex and its implications for muscle contraction. *Science.* 261: 58–65.

Rayment, I., W. R. Rypniewski, K. Schmidt-Base, R. Smith, D. R. Tomchick, M. M. Benning, D. A. Winkelmann, G. Wesenberg, and H. M. Holden. 1993b. Three-dimensional structure of myosin subfragment-1: a molecular motor. *Science.* 261:50–58.

Sase, I., H. Miyata, J. E. Corrie, J. S. Craik, and K. Kinosita, Jr. 1995a. Real time imaging of single fluorophores on moving actin with an epifluorescence microscope. *Biophys. J.* 69:323–328.

Sase, I., H. Miyata, S. Ishiwata, and K. Kinosita, Jr. 1997. Axial rotation of sliding actin filaments revealed by single- fluorophore imaging. *Proc. Natl. Acad. Sci. USA.* 94:5646–5650.

Sase, I., T. Okinaga, M. Hoshi, G. W. Feigenson, and K. Kinosita, Jr. 1995b. Regulatory mechanisms of the acrosome reaction revealed by multiview microscopy of single starfish sperm. *J. Cell Biol.* 131: 963–973.

Sellers, J. R., and B. Kachar. 1990. Polarity and velocity of sliding filaments: control of direction by actin and of speed by myosin. *Science.* 249:406–408.

Suzuki, N., H. Miyata, S. Ishiwata, and K. Kinosita, Jr. 1996. Preparation of bead-tailed actin filaments: estimation of the torque produced by the sliding force in an in vitro motility assay. *Biophys. J.* 70:401–408.

Svoboda, K., C. F. Schmidt, B. J. Schnapp, and S. M. Block. 1993. Direct observation of kinesin stepping by optical trapping interferometry. *Nature.* 365:721–727.

Taylor, K. A., H. Schmitz, M. C. Reedy, Y. E. Goldman, C. Franzini-Armstrong, H. Sasaki, R. T. Tregear, K. Poole, C. Lucaveche, R. J. Edwards, L. F. Chen, H. Winkler, and M. K. Reedy. 1999. Tomographic 3D reconstruction of quick-frozen, Ca^{2+}-activated contracting insect flight muscle. *Cell.* 99:421–431.

Toyoshima, Y. Y., S. J. Kron, E. M. McNally, K. R. Niebling, C. Toyoshima, and J. A. Spudich. 1987. Myosin subfragment-1 is sufficient to move actin filaments in vitro. *Nature.* 328:536–539.

Toyoshima, Y. Y., C. Toyoshima, and J. A. Spudich. 1989. Bidirectional movement of actin filaments along tracks of myosin heads. *Nature.* 341:154–156.

Tsuda, Y., H. Yasutake, A. Ishijima, and T. Yanagida. 1996. Torsional rigidity of single actin filaments and actin-actin bond breaking force under torsion measured directly by in vitro micromanipulation. *Proc. Natl. Acad. Sci. USA.* 93:12937–12942.

Vale, R. D., T. Funatsu, D. W. Pierce, L. Romberg, Y. Harada, and T. Yanagida. 1996. Direct observation of single kinesin molecules moving along microtubules. *Nature.* 380:451–453.

Yamada, A., N. Ishii, and K. Takahashi. 1990. Direction and speed of actin filaments moving along thick filaments isolated from molluscan smooth muscle. *J. Biochem.* 108:341–343.

Yanagida, T., M. Nakase, K. Nishiyama, and F. Oosawa. 1984. Direct observation of motion of single F-actin filaments in the presence of myosin. *Nature.* 307:58–60.

Yasuda, R., H. Noji, K. Kinosita, Jr., and M. Yoshida. 1998. F_1-ATPase is a highly efficient molecular motor that rotates with discrete 120° steps. *Cell.* 93:1117–1124.